Letter

Design of Selective Benzoxazepin PI3K# Inhibitors Through Control of Dihedral Angles

Brian Salvatore Safina, Richard L Elliott, Andrew K. Forrest, Robert A. Heald, Jeremy M. Murray, Jim Nonomiya, Jodie Pang, Laurent Salphati, Eileen M Seward, Steven Thomas Staben, Mark Ultsch, Binqing Wei, Wenqian Yang, and Daniel P. Sutherlin

ACS Med. Chem. Lett., **Just Accepted Manuscript** • DOI: 10.1021/acsmedchemlett.7b00170 • Publication Date (Web): 25 Aug 2017

Design of Selective Benzoxazepin PI3Kδ Inhibitors Through Control of Dihedral Angles

Brian S. Safina,[†]* Richard L. Elliott[§], Andrew K. Forrest[§], Robert A. Heald[§], Jeremy M. Murray[†], Jim Nonomiya[†], Jodie Pang[†], Laurent Salphati[†], Eileen M. Seward[§], Steven T. Staben[†], Mark Ultsch[†], Binqing Wei[†], Wenqian Yang[‡] and Daniel P. Sutherlin[†]

[†]Discovery Chemistry, Genentech, Inc., 1 DNA Way, South San Francisco, California 94080 [‡]ChemPartner, 998 Halei Road, Zhangjiang Hi-tech Park, Pudong New Area, Shanghai China, 201203 [§]Discovery from Charles River, 8-9 Spire Green Centre, Harlow, Essex, CM 19 5TR, United Kingdom

KEYWORDS: PI3K delta inhibitor, PI3K isoform selectivity, ligand-based design

ABSTRACT: A novel selective benzoxazepin inhibitor of PI3Kδ has been discovered. Beginning from compound **3**, an αPI3K inhibitor we utilized structure-based drug design and computational analysis of dihedral torsion angles to optimize for PI3Kδ isoform potency and isoform selectivity. Further medicinal chemistry optimization of the series led to the identification of **24**, a highly potent and selective inhibitor of PI3Kδ.

A key tenet in ligand-based drug design is optimization of ligand conformation. The preferred low energy conformation of a ligand bound to its receptor results in a lower free energy of the complex.[1] While covalently-linked ring systems effectively control three-dimensional shape, single rotatable bonds rely on more subtle non-covalent interactions to control conformation, often having the added advantage of minimal synthetic complexity and improved drug-like properties.[2,3] An understanding of the stereoelectronic and steric effects governing torsion angles of single rotatable bonds allows for maximum control of ligand conformation. Low energy torsion angles can be computationally derived and combined with data from the Cambridge Structural Database (CSD) to aid in design.[4,5,6] Combining these tactics with structure-based drug design provides a powerful tool for optimization.

a)

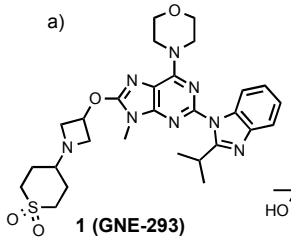

1 (GNE-293)

PI3K	Ki_{app} (nM)
α	120
β	197
δ	**0.47**
γ	103

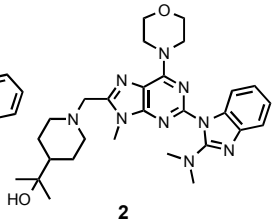

2

PI3K	Ki_{app} (nM)
α	360
β	1566
δ	**6**
γ	556

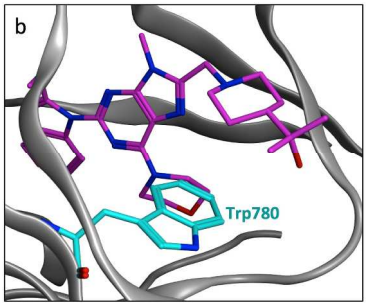

Figure 1. a) PI3Kδ potent and selective inhibitors **1** (GNE-293) and **2** derived from morpholine pyrimidine core. b) Crystal structure of compound **2** (purple) bound to PI3Kδ; PDB 4GB9.

Phosphoinositide-3-kinase delta (PI3Kδ) is a lipid kinase that has been implicated to play a key role in a variety of immune-mediated disorders such as asthma, rheumatoid arthritis and other inflammatory disease.[7] Isoform selectivity is critical to study the function of the PI3K pathway and to maximize the therapeutic indices.[8] We previously disclosed potent and selective inhibitors of PI3Kδ **1** (GNE-293) and **2** (Figure 1a), derived from a morpholine pyrimidine core. Compounds **1** and **2** are resultant from work to optimize potency and isoform selectivity via targeting specific protein-ligand interactions in an affinity pocket and a "tryptophan shelf".[9,10,11] In an effort to further expand the structural diversity of our selective PI3Kδ inhibitors we sought to capitalize on an alternative scaffold derived from our benzoxazepin class of PI3K inhibitors, exemplified by α-selective compound **3** (GDC-0326, Figure 2a).[12]

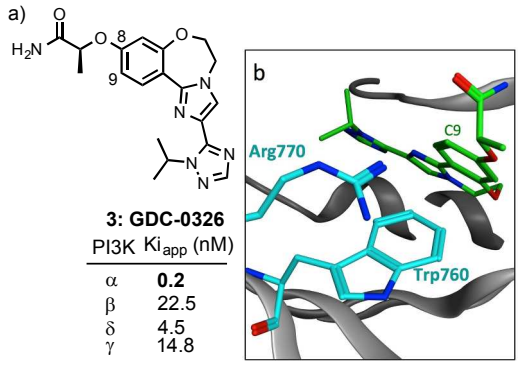

Figure 2. a) Compound **3** (GDC-0326) αPI3K isoform inhibitor derived from the benzoxazepin core. b) Crystal structure of compound **3** (green) bound to PI3Kα (cyan); PDB 5DXT.

Our strategy to optimize the benzoxazepin scaffold (**3**) towards a PI3Kδ-selective inhibitor was very attractive for several reasons. Firstly, the benzoxazepin scaffold was the result of extensive ADME optimization and thus already possessed favorable drug like properties.[13,14] Secondly, **3** was already potent against PI3Kδ making isoform selectivity the starting challenge. Lastly, comparison of co-crystal structures from the morpholine pyrimidine class **2** and benzoxazepin class **3** (Figure 1b and 2b) revealed an opportunity to access a tryptophan shelf (Trp760 in PI3Kδ). This strategy had been successful for driving isoform selectivity in the optimization of the morpholine pyrimidine series where our structural rationale for PI3Kδ selectivity depended on forging favorable interactions with Trp760, which in PI3Kδ formed the base of a relatively large pocket (**2** bound in PI3Kδ, Figure 1b).[9] In PI3Kα this pocket is occluded by an arginine residue (Arg770) as depicted in Figure 2b with the co-crystal structure of GDC-0326 in PI3Kα.[12] Our strategy was to incorporate functional groups capable of interacting with Trp760 (δ) and thereby simultaneously forge offensive interactions with PI3Kα (as well as β and γ) where large residues occlude a "tryptophan shelf".[9] Further analysis of the crystal structure suggested that the best vector to interact with the Trp shelf to increase selectivity was from the C9-aryl position of the benzoxazepin core (Fig 2b).

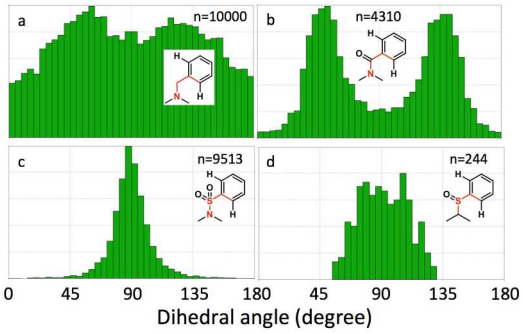

Figure 3. Dihedral angle histogram from the The Cambridge Structural Database (Mogul CSD v5.37) for a) methylene linker, b) amide linker, c) sulfonamide linker and d) sulfoxide linker.

Accordingly, four functional groups with a range of rotameric preferences were computationally analyzed (methylene, amide, sulfonamide and sulfoxide) to identify a preferred rotamer capable of extending from the C9-aryl benzoxazepin position to maximize interactions with Trp760.[9] A statistical analysis of the torsion angles for each generic functional group from the CSD is depicted in Figure 3a-d and the results were used as a selection criteria. Each histogram represents the observed frequency of torsion angles (0° to 180°) for a particular functional group. In addition to identifying the preferred rotamer from the observed frequency (number of hits), one can also infer relative energy differences between rotamers. For example, (Figure 3a) a CSD search of fragments containing a benzyl amine moiety, not surprisingly shows a relatively flat histogram and weak rotameric preference, implying low rotational barriers and fewer restrictive conformations. Substitution of the methylene with a carbonyl to yield an amide moiety produced a histogram with sharp peaks at 45° (and 135°) implying higher rotational barriers and consequently, a more restrictive conformation (Figure 3b). In contrast, a sulfonamide moiety predominantly yields 90° torsion angles (Figure 3c), where both the aromatic p orbital and nitrogen lone pair bisect the sulfonyl (O=S=O) angle. Again, the precise rotamer conformation is further dictated by *N*-alkyl substitution and aromatic ortho substitution. Examination of a sulfoxide moiety in the CSD yielded dramatically less examples, nonetheless, a pattern is emergent (Figure 3d) where torsion angles between 75° and 105° were subtly preferred.

We synthesized an assortment of molecules (**4** – **9**) containing a t-Bu piperazine moiety attached at the C-9 aryl position, varying only the torsion functionality (See Supplemental Information). Past experience taught us that forging both a hydrophobic and cation-pi

interaction with Trp760 favored increased potency and selectivity.[9] Comparing examples **4** and **5** (Table 1), demonstrated that a highly basic ^{t}Bu piperazine increased biochemical potency for PI3Kδ ten fold. While not optimal in terms of α/δ selectivity (22 fold), the t-Bu piperazine served as an appropriate substituent to build SAR around torsion angle preferences.

Table 1. SAR of C9-aryl benzoxazepin around torsion angle preferences to achieve selectivity, compounds **4-9.**

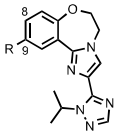

Entry	R	Ki_{app} (nM) PI3K-δ	fold selectivty α/δ	preferred torsion angle(s) from CSD	HLM[a]	cLogD[b]
4	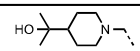	20	3	na	6.8	2.7
5	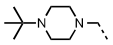	2.5	22	na	9.7	2.3
6	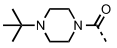	1.7	23	45°, 135°	14	2.5
7	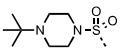	1.2	78	90°	20	2.6
8	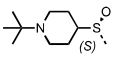	0.81	184	75° - 105°	17	2.6
9	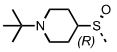	12	58	75° - 105°	12	2.6

[a] Human hepatic clearance predicted from human liver microsomes (HLM = stable <6, moderate 6-15, labile >15 mL/min/kg). [b] MoKa v.2.6.5.

Not surprisingly, compounds **5** and **6** did not have high α/δ selectivity (22 and 23 fold, respectively) and was consistent with data found in the CSD (Figure 3a and 3b) depicting low barriers of rotation for **5** and a preferred 45° torsion angle for **6** which is not compatible with the binding pose of the *N*-substituted piperazine. Interestingly, selectivity increased with sulfonamide **7** (α/δ = 78 fold) bearing a preferred torsion angle of 90°. The *S*-isomer of

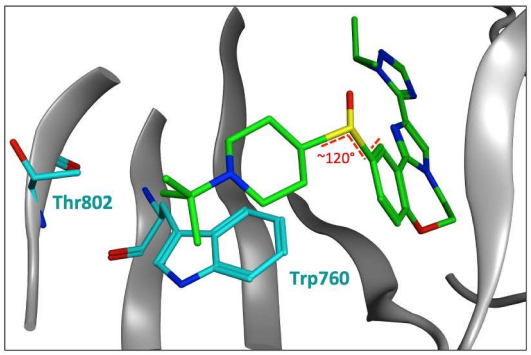

Figure 4. 2.1Å co-crystal structure of compound **8** bound to PI3Kγ · · · · · · · · · · · · · (used as a surrogate for PI3Kδ).

sulfoxide **8** yielded very high selectivity (α/δ = 184 fold) while the opposite *R*-isomer **9** was moderately selective and accompanied by erosion in PI3Kδ potency (PI3Kδ = 11.6 nM). The *S*-isomer of sulfoxide **8** suggested two possible explanations for increased potency and selectivity, 1) a preferred rotamer is either 75° or 105°, and/or 2) the sulfoxide moiety itself was responsible for making new favorable (δ) and/or unfavorable (PI3Kα) interactions. A co-crystal structure of the *S*-isomer **8** in PI3Kγ (0.596 μM IC_{50} in PI3Kγ) revealed an experimental torsion angle of ~120°, effectively positioning the ^{t}Bu piperazine moiety to interact with Trp760, making a favorable cation-pi interaction (Figure 4). We were confident that the preferred torsion angle was in the vicinity of 120°.

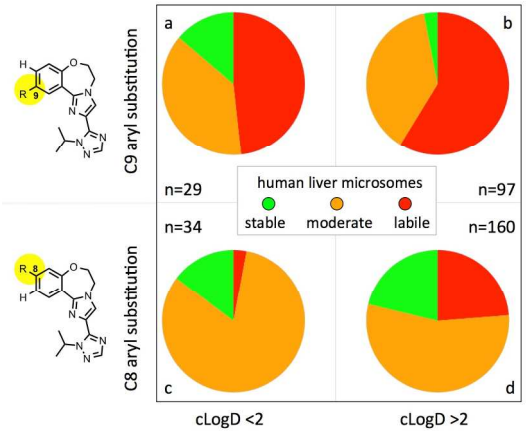

Figure 5. Human liver microsome stability and calculated lipohilicity for C8 vs C9 aryl substitution.

For our next round of design we incorporated knowledge of lipophilicity and substituent effects on metabolism in combination with torsion control. *In vitro* human liver microsomes (HLM, Table 1) indicated a range of predicted stabilities from moderate to labile, with our most potent and selective compound **8** predicted to have high clearance (17 mL/min/kg). Analysis of HLM data across the benzoxazepin series divided into four bins (C8 vs C9 aryl substitution and cLogD <2 vs cLogD >2) revealed trends that would influence future designs (Figure 5a-d). HLM data showed a higher percentage of stable to moderate stability for C8-aryl substituted benzoxazepin (Figure 5c and 5d). Furthermore, lipophilicity was a potential contributor to HLM stability and suggested compounds with a cLogD <2 could further reduce the percentage of compounds exhibiting labile human liver microsomal stability (Figure 5c) to <5% when in conjunction with C8 substitution.

These key learnings were applied towards further optimization and our goal was to design a series of molecules to meet the following three criteria. First, target a dihedral torsion angle of approximately 120° aimed at restricting the conformation to interact with Trp760. Secondly, design compounds that contain C8-aryl substitution to block potential metabolism. Lastly, design targets in the desirable lipophilicity range (cLogD <2) towards improving predicted human liver microsomal stability.

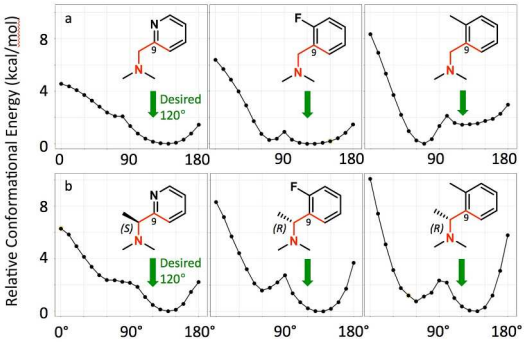

Figure 6. Computationally derived torsion scans for hypothetical linkers a) C8-aryl substitution and b) C8-aryl and methylene substitution. Dihedrals were scanned from 0 to 360 degrees in 10-degree increments (See Supplemental Information for computational method).

Toward this end, a handful of bis-C8,C9-aryl substituted benzoxazepin fragments were evaluated computationally to derive energy/torsion angle plots (Figure 6a). Preliminary designs showed promise in reinforcing our desired torsion angle of ~120°, especially for the C-8 fluorine and methyl substituted analogs. A more pronounced torsion restriction was achieved by the addition of a methyl group to the methylene benzylic C-9 position (Figure 6b). The methyl substituent alleviated 1,3-strain with the corresponding C-8 substitution.

Analog synthesis was carried out incorporating the three newly designed fragments along with their corresponding enantiomers (See Supplemental Information). The biochemical potency and selectivity is shown in Table 2.

Table 2. Potency and selectivity for C9 and C8 substituted benzoxazepins, compounds **10-15**.

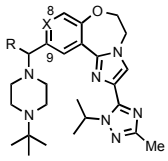

Entry	X	R	Ki_{app} (nM) PI3K-δ	*fold selectivty* α/δ
10	C-Me	(*R*)-Me	0.48	109
11	C-Me	(*S*)-Me	0.88	27
12	C-F	(*R*)-Me	0.78	479
13	C-F	(*S*)-Me	2.4	102
14	N	(*R*)-Me	2.8	28
15	N	(*S*)-Me	1.9	113

Gratifyingly, PI3Kδ selectivity for all three pairs of enantiomers, e.g. **10** *R*-Me α/δ = 109 and **15** *S*-Me α/δ = 113 were greater than 100 fold. Most notably, fluorine substituent, as in **12**, achieved 479 fold α/δ selectivity. Further profiling of compounds **10**, **12** and **15** (Table 3) revealed an improved human liver microsomal stability for pyridinyl compound **15** (<3.9 mL/min/kg). Compound **15** also possessed the lowest cLogD (1.29) and still maintained high permeability (MDCK A to B = 10 x 10^{-6} cm/s) along with excellent human whole blood potency (HWB = 28 nM).[15]

Table 3. Human liver microsome stability, permeability and human whole blood potency for compounds **10-15**.

Entry	cLogD[a]	HLM[b]	MDCK[c] Papp A to B x10^{-6} cm/s	CD69 HWB[d] IC_{50} (nM)
10	2.3	8.4	14.2	4.9
12	1.9	15	13.6	15
15	1.3	<3.9	10	28

[a] MoKa v.2.6.5. [b]Human hepatic clearance predicted from human liver microsomes (stable <6, moderate 6-15, labile >15 mL/min/kg). [c] Apparent permeability in MDCK transwell culture. low <1, moderate 1-10, high >10. [d]See reference 14.

In summary, we have discovered a novel benzoxazepin class of selective PI3Kδ inhibitors. Through the aid of structure based design we successfully applied our selectivity hypothesis, derived from a structurally diverse morpholine pyrimidine class, to target a unique "tryptophan shelf" in PI3Kδ. Application to the benzoxazepin class was achieved by evaluating dihedral torsion angles both computationally and experimentally, in an iterative process, to identify a low energy conformation capable of achieving the desired potency and selectivity. Ultimately, compound **15** containing bis C8, C9-aryl substitution and a cLogD <2 yielded a potent and selective PI3Kδ inhibitor with low predicted human clearance, high

permeability and excellent human whole blood potency.

AUTHOR INFORMATION

Corresponding Author

*Brian S. Safina. Tel.: +1 650-467-7450, e-mail address: bsafina@gene.com

Author Contributions

All authors have given approval to the final version of the manuscript.

Notes

The authors declare no competing financial interest.

ACKNOWLEDGMENT

We thank Mengling Wong for purification of analogs.

ABBREVIATIONS

PI3K, phosphoinositide-3-kinase

REFERENCES

1. Yang, S.Y. Pharmacophore modeling and applications in drug discovery: challenges and recent advances. Drug Discovery Today, **2010**, *15*, 444-450.
2. Gillis, E. P.; Eastman, K. J.; Hill, M. D.; Donnelly, D. J.; Meanwell, N. A. Applications of Fluorine in Medicinal Chemistry. *J. Med. Chem.* **2015**, *58* (21), 8315–8359.
3. Beno, B. R.; Yeung, K.-S.; Bartberger, M. D.; Pennington, L. D.; Meanwell, N. A. A Survey of the Role of Noncovalent Sulfur Interactions in Drug Design. *J. Med. Chem.* **2015**, *58*, 4383–4438.
4. Groom, C. R.; Bruno, I. J.; Lightfoot, M. P.; Ward, S. C. Feature Articles. Acta Cryst. 2016, B72, 171-179.
5. Allen, F. H. The Cambridge Structural Database: A Quarter of a Million Crystal Structures and Rising. *Acta Crystallogr., Sect. B: Struct. Sci.* **2002**, B58, 380-388.
6. Brameld, K. A.; Kuhn, B.; Reuter, D. C.; Stahl, M. Small Molecule Conformational Preferences Derived From Crystal Structure Data. a Medicinal Chemistry Focused Analysis. *J. Chem. Inf. Model.* **2008**, *48*, 1–24.
7. Cushing, T. D.; Metz, D. P.; Whittington, D. A.; McGee, L. R. PI3Kδ and PI3Kγ as Targets for Autoimmune and Inflammatory Diseases. *J. Med. Chem.* **2012**, *55*, 8559–8581.
8. Hennessy, B. T.; Smith, D. L.; Ram, P. T.; Lu, Y.; Mills, G. B. Exploiting the PI3K/AKT Pathway for Cancer Drug Discovery. *Nat Rev Drug Discov* **2005**, *4*, 988–1004.
9. Sutherlin, D. P.; Baker, S.; Bisconte, A.; Blaney, P. M.; Brown, A.; Chan, B. K.; Chantry, D.; Castanedo, G.; DePledge, P.; Goldsmith, P.; Goldstein, D. M.; Hancox, T.; Kaur, J.; Knowles, D.; Kondru, R.; Lesnick, J.; Lucas, M. C.; Lewis, C.; Murray, J.; Nadin, A. J.; Nonomiya, J.; Pang, J.; Pegg, N.; Price, S.; Reif, K.; Safina, B. S.; Salphati, L.; Staben, S.; Seward, E. M.; Shuttleworth, S.; Sohal, S.; Sweeney, Z. K.; Ultsch, M.; Waszkowycz, B.; Wei, B. Potent and Selective Inhibitors of PI3Kδ: Obtaining Isoform Selectivity From the Affinity Pocket and Tryptophan Shelf. *Bioorg. Med. Chem. Lett.* **2012**, *22*, 4296–4302.
10. Murray, J. M.; Sweeney, Z. K.; Chan, B. K.; Balazs, M.; Bradley, E.; Castanedo, G.; Chabot, C.; Chantry, D.; Flagella, M.; Goldstein, D. M.; Kondru, R.; Lesnick, J.; Li, J.; Lucas, M. C.; Nonomiya, J.; Pang, J.; Price, S.; Salphati, L.; Safina, B.; Savy, P. P. A.; Seward, E. M.; Ultsch, M.; Sutherlin, D. P. Potent and Highly Selective Benzimidazole Inhibitors of PI3-Kinase Delta. *J. Med. Chem.* **2012**, *55*, 7686–7695.
11. Safina, B. S.; Sweeney, Z. K.; Li, J.; Chan, B. K.; Bisconte, A.; Carrera, D.; Castanedo, G.; Flagella, M.; Heald, R.; Lewis, C.; Murray, J. M.; Nonomiya, J.; Pang, J.; Price, S.; Reif, K.; Salphati, L.; Seward, E. M.; Wei, B.; Sutherlin, D. P. *Bioorg. Med. Chem. Lett.* **2013**, *23*, 4953–4959.
12. Heffron, T. P.; Heald, R. A.; Ndubaku, C.; Wei, B.; Augistin, M.; Do, S.; Edgar, K.; Eigenbrot, C.; Friedman, L.; Gancia, E.; Jackson, P. S.; Jones, G.; Kolesnikov, A.; Lee, L. B.; Lesnick, J. D.; Lewis, C.; McLean, N.; Mörtl, M.; Nonomiya, J.; Pang, J.; Price, S.; Prior, W. W.; Salphati, L.; Sideris, S.; Staben, S. T.; Steinbacher, S.; Tsui, V.; Wallin, J.; Sampath, D.; Olivero, A. G. The Rational Design of Selective Benzoxazepin Inhibitors of the A-Isoform of Phosphoinositide 3-Kinase Culminating in the Identification of (S)-2-((2-(1-

Isopropyl-1 H-1,2,4-Triazol-5-Yl)-5,6-Dihydrobenzo[F]Imidazo[1,2-D][1,4]Oxazepin-9-Yl)Oxy)Propanamide (GDC-0326). *J. Med. Chem.* **2016**, *59*, 985–1002.

13. Ndubaku, C. O.; Heffron, T. P.; Staben, S. T.; Baumgardner, M.; Blaquiere, N.; Bradley, E.; Bull, R.; Do, S.; Dotson, J.; Dudley, D.; Edgar, K. A.; Friedman, L. S.; Goldsmith, R.; Heald, R. A.; Kolesnikov, A.; Lee, L.; Lewis, C.; Nannini, M.; Nonomiya, J.; Pang, J.; Price, S.; Prior, W. W.; Salphati, L.; Sideris, S.; Wallin, J. J.; Wang, L.; Wei, B.; Sampath, D.; Olivero, A. G. Discovery of 2-{3-[2-(1-Isopropyl-3-Methyl-1H-1,2-4-Triazol-5-Yl)-5,6-Dihydrobenzo[F]Imidazo[1,2-D][1,4]Oxazepin-9-Yl]-1H-Pyrazol-1-Yl}-2-Methylpropanamide (GDC-0032): a B-Sparing Phosphoinositide 3-Kinase Inhibitor with High Unbound Exposure and Robust in Vivo Antitumor Activity. *J. Med. Chem.* **2013**, *56*, 4597–4610.
14. Staben, S. T.; Ndubaku, C.; Blaquiere, N.; Belvin, M.; Bull, R. J.; Dudley, D.; Edgar, K.; Gray, D.; Heald, R.; Heffron, T. P.; Jones, G. E.; Jones, M.; Kolesnikov, A.; Lee, L.; Lesnick, J.; Lewis, C.; Murray, J.; McLean, N. J.; Nonomiya, J.; Olivero, A. G.; Ord, R.; Pang, J.; Price, S.; Prior, W. W.; Rouge, L.; Salphati, L.; Sampath, D.; Wallin, J.; Wang, L.; Wei, B.; Weismann, C.; Wu, P. *Bioorg. Med. Chem. Lett.* **2013**, *23*, 2606–2613.
15. Baker, S. J.; Goldsmith, P.; Hancox, T. C.; Pegg, N. A.; Price, S.; Shuttleworth, S. J. WO 2007122410 A1.

Abstract graphic